The Journals of Gerontology, Series A: Biological Sciences and Medical Sciences, 2024, **79**(1), 1–8
https://doi.org/10.1093/gerona/glad182
Advance access publication 1 August 2023
Research Article

Structural Network Efficiency Predicts Conversion to Incident Parkinsonism in Patients With Cerebral Small Vessel Disease

Mengfei Cai, MD, PhD,[1,2] Mina A. Jacob, MD,[2] José Marques, PhD,[3] David G. Norris, PhD,[3] Marco Duering, MD,[4] Rianne A.J. Esselink, MD, PhD,[2] Yuhu Zhang, MD, PhD,[5] Frank-Erik de Leeuw, MD, PhD,[2] and Anil M. Tuladhar, MD, PhD[2,*]

[1]Department of Neurology, Guangdong Cardiovascular Institute, Guangdong Neuroscience Institute, Guangdong Provincial People's Hospital, Guangdong Academy of Medical Sciences, Southern Medical University, Guangzhou, People's Republic of China.
[2]Department of Neurology, Radboud University Medical Center, Donders Institute for Brain, Cognition and Behaviour, Nijmegen, The Netherlands.
[3]Donders Institute for Brain, Cognition and Behaviour, Radboud University, Nijmegen, The Netherlands.
[4]Medical Image Analysis Center (MIAC AG) and qbig, Department of Biomedical Engineering, University of Basel, Basel, Switzerland.
[5]Department of Neurology, Guangdong Neuroscience Institute, Guangdong Provincial People's Hospital (Guangdong Academy of Medical Sciences), Southern Medical University, Guangzhou, People's Republic of China.

*Address correspondence to: Anil M. Tuladhar, MD, PhD. E-mail: Anil.Tuladhar@radboudumc.nl

Decision Editor: Lewis A. Lipsitz, MD, FGSA (Medical Sciences Section)

Abstract

Background: To investigate whether structural network disconnectivity is associated with parkinsonian signs and their progression, as well as with an increased risk of incident parkinsonism.

Methods: In a prospective cohort (Radboud University Nijmegen Diffusion Tensor and Magnetic Resonance Cohort study) consisting of 293 participants with small vessel disease (SVD), we assessed parkinsonian signs and incident parkinsonism over an 8-year follow-up. In addition, we reconstructed the white matter network followed by graph-theoretical analyses to compute the network metrics. Conventional magnetic resonance imaging markers for SVD were assessed.

Results: We included 293 patients free of parkinsonism at baseline (2011), with a mean age 68.8 (standard deviation [*SD*] 8.4) years, and 130 (44.4%) were men. Nineteen participants (6.5%) developed parkinsonism during a median (*SD*) follow-up time of 8.3 years. Compared with participants without parkinsonism, those with all-cause parkinsonism had higher Unified Parkinson's Disease Rating scale (UPDRS) scores and lower global efficiency at baseline. Baseline global efficiency was associated with UPDRS motor scores in 2011 ($\beta = -0.047$, $p < .001$) and 2015 ($\beta = -0.84$, $p < .001$), as well as with the changes in UPDRS scores during the 4-year follow-up ($\beta = -0.63$, $p = .004$). In addition, at the regional level, we identified an inter-hemispheric disconnected network associated with an increased UPDRS motor score. Besides, lower global efficiency was associated with an increased risk of all-cause and vascular parkinsonism independent of SVD markers.

Conclusions: Our findings suggest that global network efficiency is associated with a gradual decline in motor performance, ultimately leading to incident parkinsonism in the elderly with SVD. Global network efficiency may have the added value to serve as a useful marker to capture changes in motor signs.

Keywords: Motor disturbance, Network efficiency, Parkinsonism, Small vessel disease

Cerebral small vessel disease (SVD) is radiologically identified in virtually every individual aged over 60 years old (1). It is associated with cognitive and motor decline, including gait impairment and parkinsonian signs, ultimately resulting in parkinsonism (2,3). In addition, progression of SVD markers is closely related to the worsening of motor performance over time (4). However, not all patients with SVD experience motor decline. Emerging evidence has shown that global efficiency can additionally explain the motor decline in elderly people with SVD, on top of the conventional SVD markers (5,6). Structural network analysis obtained from diffusion MRI quantifies the extent of disconnection of the structural network. Global efficiency, as one of the global network parameters, has proven to be a sensitive measure to capture brain pathological alterations in SVD (7).

Individuals with parkinsonism often exhibit mild parkinsonian signs in the prodromal stage before they clinically progress to parkinsonism (2,8). Previous cross-sectional studies have shown that patients with prevalent parkinsonism have impaired structural connectivity in contrast to healthy controls and that this was associated with worse motor

Received: March 31 2023; Editorial Decision Date: July 11 2023.

performance, that is, higher Unified Parkinson's Disease Rating scale (UPDRS) motor score (9–11).

We recently found that baseline SVD severity and progression are independently associated with incident parkinsonism (12). However, it is unknown whether structural network efficiency has the added value to capture the progression from parkinsonian signs to incident parkinsonism over time on top of SVD burden.

We hypothesized that lower structural network connectivity is related to (progression of) parkinsonian signs and increased risk of incident parkinsonism. To this end, we investigated the relation between global efficiency and regional connectivity and UPDRS motor score at the cross-sectional level and whether global efficiency was related to the UPDRS motor score longitudinally. In addition, we investigated whether global efficiency was associated with the risk of incident parkinsonism independent of MRI markers of SVD.

Materials and Methods

Study Population

This study is a part of the Radboud University Nijmegen Diffusion Tensor and Magnetic resonance Cohort (RUN DMC) study, an ongoing longitudinal prospective single-center study that investigates risk factors and clinical consequences of sporadic SVD in people aged between 50 and 85 years. A detailed description of the patient recruitment and study rationale of the RUN DMC study has been described in the study protocol (13). In short, in 2006, consecutive patients referred to the Department of Neurology between October 2002 and November 2006, were selected for participation. Inclusion criteria were (a) age between 50 and 85 years and (b) SVD on neuroimaging (white matter hyperintensities [WMHs] and/or lacunes) with the accompanying acute or subacute clinical symptoms (eg, transient ischemic attack, lacunar syndromes, cognitive and motor disturbances) of SVD. Patients who were eligible because of a lacunar syndrome were included only >6 months after the event to avoid acute effects on the outcomes.

Baseline data collection was performed in 2006, with 3 follow-ups (Follow-up 1 in 2011, Follow-up 2 in 2015, and Follow-up 3 in 2020). Due to the magnetic resonance imaging (MRI) scanner upgrade between 2006 and Follow-up 1, we only included participants with MRI data available from 2011 ($n = 293$) to 2015 ($n = 226$), who were scanned with identical MR scanners and protocols. A flowchart of this study is provided in Supplementary Figure 1.

Final data collection, including assessment of incident parkinsonism, was completed on December 9, 2020.

Of note, for ease of interpretation and description in the present study, we will refer to the 2011 assessment as **"baseline,"** and the 2015 assessment as **"follow-up."** The Medical Review Ethics Committee region Arnhem-Nijmegen approved the study and all participants gave written informed consent.

Parkinsonism Diagnostic Work-Up

We employed a standardized work-up to ascertain incident parkinsonism, comprising serial in-person visits, video examinations, and continuous follow-up of medical records.

The presence of parkinsonian signs was evaluated during the in-person follow-up assessments (2011, 2015, 2020) by well-trained residents in neurology by using the motor part of the UPDRS motor score (14), verified by a movement disorders specialist (R.A.J.E.). Parkinsonism was defined as the presence of bradykinesia and at least one of the 3 following signs: tremor, rigidity, or gait and postural instability, according to the UK Parkinson's Disease Society Brain Bank criteria (15). We assessed the presence of these 4 signs based on scores derived from the UPDRS-m, including limb bradykinesia (based on 8 items: right and left finger taps, handgrip, hand pronation-supination, and leg agility), rigidity (based on 5 items: rigidity of neck and the 4 extremities), tremor (based on 7 items: rest tremor of lip/chin and 4 extremities and action tremor of both arms), and parkinsonian gait (based on 5 items: arise from chair, posture, gait, postural stability, and body bradykinesia). We considered bradykinesia as present when ≥1 item on limb bradykinesia had a score of ≥2(14–16), to guarantee a high sensitivity of this main symptom of parkinsonism. The other 3 signs (tremor, rigidity, and gait and postural instability) were considered present when the participant had either ≥2 items with a score of ≥1, or 1 item with a score of ≥2 in that specific category.

Participants were considered screen-positive when (1) they had bradykinesia and one or more of the other 3 signs (17), according to aforementioned criteria, or (2) had UPDRS-m score ≥10, or (3) were already diagnosed with parkinsonism by a neurologist after baseline assessment (year 2006). Screened-positive participants were invited for an additional examination by a movement disorders specialist (R.A.J.E.) to confirm the presence of parkinsonism.

Those participants who were screened positive after the in-person evaluation, but refused additional examination by the movement disorder specialist, were asked whether their UPDRS-m examination could be recorded in a video for an evaluation by a consensus panel consisting of a neurologist specialized in movement disorders (R.A.J.E.) and a neurologist specialized in cerebrovascular disease (F.E.d.L).

For patients who did not participate during follow-up (deceased or refused participation), medical records were retrieved from the general practitioners/treating physicians. Cases in whom parkinsonism was mentioned by treating physicians were evaluated again independently by the consensus panel according to a standardized structured approach, by taking into consideration all available clinical data (medical records) including medical history, medication use, all motor performance scores, neuropsychological examinations, and MRI data from all follow-up time points.

The diagnostic criteria of the UK Parkinson's Disease Society Brain Bank (21) were used for idiopathic PD (IPD), Zijlmans criteria for vascular parkinsonism (VaP) (18), and the National Institute of Neurological Disorders and Stroke—Society for Progressive Supranuclear Palsy (PSP) criteria for PSP (15). VaP requires the presence of relevant cerebrovascular disease markers on MRI, operationalized as a Fazekas score ≥2 or presence of one or more lacunes in basal ganglia or thalamus (19). Participants with drug-induced parkinsonism were excluded ($n = 4$) and not considered as "parkinsonism cases."

The date of parkinsonism onset was defined as the date on which the clinical symptoms allowed for the diagnosis. When the date of diagnosis was not exactly known (eg, if the diagnosis was made during the consensus meeting), we used the mid-point between the date of the previous research visit and the date the diagnosis was confirmed. For participants who did not develop parkinsonism, follow-up time was censored at the time of last visit, and date of most recently retrieved

medical information from general practitioner mentioning no signs or symptoms of parkinsonism, or death.

MRI Protocol

MR images were acquired on a single 1.5 Tesla scanner (Siemens, Magnetom Avanto). The protocol consisted of the following whole-brain scans: T1-weighted 3D Magnetization Prepared RApid Gradient Echo (MPRAGE) sequence (TR/TE/TI: 2250/2.95/850 ms, isotropic voxel size: 1.0 mm^3), Fluid-attenuated inversion recovery (FLAIR; TR/TE/TI: 14240/89/2200 ms, voxel size: 1.2 × 1.0 × 2.5 mm, interslice gap 0.5 mm), T2*-weighted gradient echo sequence (voxel size: 1.3 × 1.0 × 5.0 mm; interslice gap 1.0 mm) and a DTI sequence (TR/TE: 10200/95, isotropic voxel size: 2.5 mm^3), 7 unweighted scans, 61 diffusion-weighted scans at b = 900 s/mm^2. Full acquisition details have been described previously (20).

Conventional MRI Markers of SVD

The rating of SVD markers was based on the STandards for ReportIng Vascular changes on nEuroimaging (STRIVE) criteria (21). WMH was segmented semi-automatically using FLAIR and T1 sequences as described previously (22). All segmentations were visually inspected for segmentation errors by one trained rater, who was blinded for clinical data. WMH volumes were normalized to intracranial volume. Lacunes were manually rated on T1-weighted and FLAIR images, and microbleeds on the T2*-weighted images. These markers were rated by 2 trained raters, followed by a consensus meeting. Intra- and interrater reliability were excellent, that is, weighted kappa of 0.87 and 0.95 for lacunes and 0.85 and 0.86 for microbleeds (23). Gray matter volume (GMV) and white matter volume (WMV) were calculated employing Statistical Parametric Mapping 12 (SPM, https://www.fil.ion.ucl.ac.uk/spm). SPM12 unified segmentation on T1 sequences and was computed by summing all voxels belonging to tissue class multiplied by voxel volume (ml). Total brain volume was calculated by summing GMV and WMV.

DTI Analysis

A local principal component analysis filter was used to denoise the raw diffusion-weighted data (24). We corrected for cardiac and head motion as well as eddy currents by using the PATCH (Patching ArTefacts from Cardiac and Head motion) algorithm as reported previously (25). This well-established method was shown to be robust and sensitive to detect and correct the most frequently occurring DWI artifacts with excellent performance. Susceptibility distortions were unwrapped by normalizing the images to the T1 images in the phase-encoding direction via SPM12. We then used FMRIB Software Library (FSL) to extract brain tissue and calculate the diffusion tensor (26) and in-house software to conduct whole-brain deterministic tractography by seeding from a 0.5 mm^3 grid, with streamlines terminated when the angle between principal eigenvectors >40° or fractional anisotropy (FA) <0.2 (27).

Structural Network Construction

We parcellated each brain into 45 regions per hemisphere using the automatic anatomical label (AAL) template (28). Cerebellar regions were excluded because the tractography technique employed in this study is unsuitable for tracing cerebellar connections. T1-weighted images were linearly registered to the b0-image by FMRIB's Linear Image Registration Tool (FLIRT, part of FSL) (29) and nonlinearly registered to the Montreal Neurological Institute 152 template using Advanced Normalization Tools (30). These transformations were combined to register the AAL template to each subject's diffusion space.

Connectivity weights were ascribed to edges to capture information about connection strength. Edge weights (W_{ij}) were computed for each edge based on the lengths (in mm), l of the set of N streamlines with endpoints terminating in each pair of nodes i and j, $W_{ij} = \frac{1}{2}\sum_{m=0}^{N}\frac{1}{l_m}$, modified from Hagmann et al. (31). This includes a scaling factor to correct for the number of seeds per millimeter of tract length. This weighting technique has the benefit of simple interpretation; that is, W_{ij} represents the seeding-corrected number of unique streamlines passing between i and j. Edges were thresholded at W_{ij} = 1 to minimize noise-related false positives (32). This resulted in a weighted 90 × 90 connectivity matrix for each individual.

Of note, we did not threshold the corresponding networks to a certain density given others have already reported the effect of density thresholding and found that networks weighted by FA might be less prone to network density effects (33).

Network Measures

We used the brain connectivity toolbox (http://www.brain-connectivity-toolbox.net) to compute graph-theoretical measures. We calculated the following 4 global network measures: density, total network strength, local, and global efficiency. Efficiency between 2 regions is expressed as the inverse of the shortest path length between 2 regions. The shortest path length refers to the minimum number of weighted connections between 2 regions. Global efficiency is defined as the average efficiency for all node pairs, reflecting the extent to which information communication is globally integrated in the network (34). Because the network parameters are highly correlated with each other, we used the global efficiency as a marker of the network disruption, as applied in other studies (35).

Peak Width of Skeletonized Mean Diffusivity (PSMD)

PSMD is a fully automated, and robust SVD imaging marker, calculated with the PSMD tool provided at http://www.psmd-marker.com(36).

Statistical Analysis

Clinical and imaging characteristics of participants are presented as mean ± standard deviation (*SD*) for normally distributed data, median, and interquartile ranges (IQR) for the skewed distributed parameters. Mann–Whitney *U*-test, *t*-test, or χ^2 were used as appropriate to compare baseline characteristics between participants with and without parkinsonism, between idiopathic Parkinson's disease and vascular parkinsonism group.

Whole-brain network analysis

To examine the cross-sectional association between global efficiency and UPDRS motor score at baseline, we used multivariable linear regression, while adjusting for age, sex, SVD markers, that is, number of lacunes and microbleeds, WMH volume, and total brain volume.

To investigate the relation between global efficiency and UPDRS longitudinally, we used multivariable linear regression to examine the relationship between baseline global efficiency in 2011 and (1) UPDRS motor score in 2015; (2) change in UPDRS motor score between the year 2011 and 2015. Adjustments were made for age, sex, SVD markers, that is, number of lacunes and microbleeds, WMH volume, and total brain volume at baseline.

Regional network analysis

To examine the regional differences in structural connectivity between all-cause parkinsonism group and non-parkinsonism group at baseline (2011), we used the Network-Based Statistic (NBS) toolbox (nitrc.org/projects/nbs), while adjusting for age and sex. A set of supra-threshold connections with statistically significant association were defined as $t > 1.65$ (corresponding to p-uncorrected < .05). In addition, we explored the region-specific network disruption associated with UPDRS score at baseline with NBS toolbox ($t > 1.65$ corresponding to p-uncorrected < .05). Multiple comparisons were controlled using family-wise error rate and data were permuted 5000 times.

Global efficiency and incident parkinsonism

We calculated the cumulative incidence of all-cause parkinsonism during the follow-up, censoring at death or the last available follow-up. The cumulative incidence of all-cause parkinsonism was estimated using Kaplan–Meier analysis, stratified by global efficiency in quartiles. Differences between the lowest and highest quartile were compared by log-rank test.

To investigate whether baseline global efficiency and change in global efficiency (2011–2015) are associated with all-cause parkinsonism incidence after the Follow-up 1 (2011), we used Cox regression models to calculate the hazard ratios (HRs) and 95% confidence interval (CI) after adjustment for age, sex, SVD markers, that is, number of lacunes and microbleeds, WMH volume and total brain volume, PSMD at baseline. In view of the potential competing risk of death, we performed Cox regression using competing risk models (Fine-Gray sub-distribution hazard model) (37). Schoenfeld residuals were investigated to verify the proportionality of hazards. There were no indications that the proportional hazards assumption was violated.

The rationale of utilizing Fine-Gray sub-distribution hazard model is that during the 8-year long-term follow-up, both incident parkinsonism and death can occur. Our primary outcome is incident parkinsonism, while death would preclude the occurrence of incident parkinsonism. Fine-Gray Cox model is intended to estimate the sub-distribution hazard, which represents the instantaneous risk of experiencing a specific event (parkinsonism) while accounting for the presence of competing risk (death). It has the advantage of considering both the occurrence of the event of interest and the occurrence of other competing events, thus providing a more comprehensive analysis of the cumulative incidence of each event. In addition, we also performed a cox regression model, while treating the death as a censoring variable.

Two-tailed p values of <.05 were considered statistically significant. Unless otherwise specified, all statistical analyses were carried out in *R*, version 4.1.1.

Results

We included 293 patients free of parkinsonism at baseline (2011), with a mean age of 68.8 (*SD* 8.4) years, and 130 (44.4%) were men. In total, 19 participants (6.5%) developed parkinsonism during a median (*SD*) follow-up time of 8.3 (IQR 7.8–8.7) years, resulting in an incidence rate of 3.34 (95% CI 6.7–11.8) per 1000 person-years.

Network Difference Between Those With and Without Parkinsonism

Compared with participants without parkinsonism, patients with all-cause parkinsonism had higher UPDRS scores and lower global efficiency at baseline (Table 1).

At the regional level, a disconnected edge-wise network was found in participants with all-cause parkinsonism compared with the non-parkinsonism group, revealing a topologic cluster with edges of frontofrontal, frontotemporal, and frontoparietal connections. Of 48 disrupted connections (eg, edges), 34 were inter-hemispheric (70.8%; Supplementary Figure 2).

Associations Between Global Efficiency and UPDRS Motor Scores

Baseline global efficiency was associated with UPDRS motor score in 2011 and 2015 (β = −0.47, p value < .001; β = −0.84, p value < .001, respectively), as well as the changes in UPDRS score during the 4-year follow-up (β = −0.38, p value = .004; Table 2). Change in global efficiency was, however, not associated with change in UDPRS score between 2011 and 2015, while adjusting for age and sex (β = 0.12, p = .638).

In addition, at the regional level, we identified an inter-hemispheric decreased subnetwork associated with increased UPDRS motor score, passing through all major subdivisions of the corpus callosum, involving frontal, temporal, parietal, and occipital lobes. Of 135 disrupted connections (eg, edges), 81 were inter-hemispheric (60%; Figure 1).

Global Efficiency and Incident Parkinsonism

The cumulative risk for all-cause parkinsonism was highest in participants with the lowest quartile of global efficiency at baseline (Figure 2). After adjustment for age, sex, number of lacunes and microbleeds, WMH volume, and total brain volume, lower global efficiency was associated with an increased risk of all-cause parkinsonism (HR [95% CI]): 0.73 per 1 – *SD* increase [0.56–0.96]) and vascular parkinsonism (HR [95% CI]): 0.58 per 1 – *SD* increase [0.40–0.84]), when treating death as a competing risk (Table 3). We also treated death as a censoring variable and obtained similar findings (Supplementary Table 1).

After additional adjustment for PSMD, lower global efficiency remained significantly associated with an increased risk of all-cause parkinsonism (HR [95% CI]: 0.74 per 1-SD increase [0.54–0.96]) and vascular parkinsonism (HR [95% CI]: 0.57 per 1-SD increase [0.37–0.89]; Supplementary Table 2).

However, changes in global efficiency were not associated with all-cause, vascular parkinsonism and idiopathic Parkinson's disease (Table 3).

Discussion

In this prospective study, we showed that lower global efficiency was associated with lower motor performance cross-sectionally and longitudinally in elderly individuals with SVD. In addition, the disruption of structural connectivity, on top of SVD markers, was associated with an increased risk of incident parkinsonism over an 8-year follow-up, reflecting the

Table 1. Baseline (2011) Characteristics of the Study Population

N = 293	All-Cause Parkinsonism (*n* = 19)	Non-Parkinsonism (*n* = 274)	*p* Value	Idiopathic PD (*n* = 8)	Vascular Parkinsonism (*n* = 11)	*p* Value
Demographics						
Age (mean (SD))	70.60 (8.92)	68.67 (8.40)	.335	66.52 (9.20)	73.57 (7.81)	.088
Sex, Male (%)	5 (26.3)	125 (45.6)	.162	2 (25.0)	3 (27.3)	1.000
UPDRS motor score						
UPDRS motor (mean (SD))	6.89 (6.42)	3.20 (4.26)	**<.001**	4.25 (4.83)	8.82 (6.94)	.129
Gait/balance (mean (SD))	1.37 (1.77)	0.66 (1.40)	**.038**	0.62 (0.74)	1.91 (2.12)	.121
Bradykinesia (mean (SD))	2.89 (2.69)	1.47 (1.96)	**.003**	1.75 (1.58)	3.73 (3.07)	.115
Rigidity (mean (SD))	0.95 (1.81)	0.48 (1.01)	**.067**	0.50 (1.07)	1.27 (2.20)	.373
Tremor (mean (SD))	1.05 (1.68)	0.37 (0.91)	**.004**	1.00 (2.14)	1.09 (1.38)	.911
Network metrics						
Global efficiency (mean (SD))	8.07 (2.72)	10.27 (2.45)	**<.001**	10.11 (2.30)	6.59 (1.98)	**.002**
SVD markers						
WMH (median [IQR])	7.92 [2.22, 25.96]	2.96 [1.29, 8.58]	.074	2.34 [1.25, 5.56]	9.57 [5.22, 38.83]	**.032**
Lacune, presence, n (%)	4 (21.1)	34 (12.4)	.465	0 (0.0)	4 (36.4)	.177
Microbleeds, presence (%)	4 (21.1)	55 (20.1)	1.000	1 (12.5)	3 (27.3)	.834
TBV (mean (SD))	1037.00 (96.24)	1095.19 (174.53)	.152	1037.16 (96.38)	1036.89 (100.84)	.995

Notes: Data represent number of participants (%), mean ± *SD*. Bold values means significant statistically. SD = standard deviation; SVD = small vessel disease; TBV = total brain volume; UPDRS = Unified Parkinson's Disease Rating scale; WMH = white matter hyperintensity.

Table 2. Associations Between Global Efficiency and UPDRS Motor Scores

	UPDRS 2011			UPDRS 2015			Delta UDPRS 2011–2015		
Variables	Beta	95% CI	*p* Value	Beta	95% CI	*p* Value	Beta	95% CI	*p* Value
Baseline GE	−0.47	−0.72 to −0.22	**<.001**	−0.84	−1.15 to −0.54	**<.001**	−0.38	−0.63 to −0.13	**.003**

Notes: All 3 models were adjusted for age, sex, number of lacunes and microbleeds, white matter hyperintensity volume, and total brain volume. Bold values means significant statistically. CI = confidence interval; GE = global efficiency; UPDRS = Unified Parkinson's Disease Rating scale.

Figure 1. Subnetwork related to UPDRS motor score. The disconnections

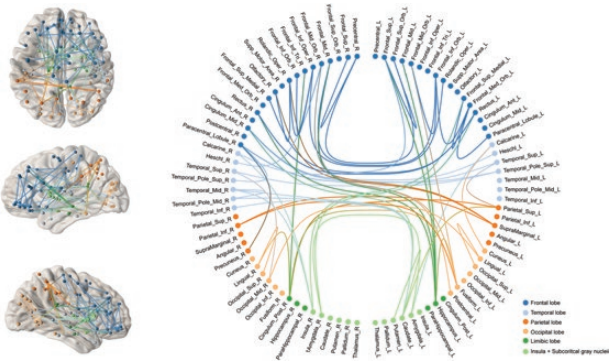

in structural connectivity are represented by brain connectivity maps (*t*-statistic threshold, 1.65) and a circular connectogram. Brain regions are grouped on the connectogram circumference according to lobes (frontal, temporal, parietal, occipital, limbic, and subcortical gray nuclei). Left hemisphere nodes are shown on the right side of the connectogram. Brain connectivity maps and circular connectogram were generated using NeuroMArVL (http://immersive.erc.monash.edu.au/neuromarvl). UPDRS = Unified Parkinson's Disease Rating scale.

crucial role of brain structural disconnection in the progression of parkinsonian signs over time.

Using NBS analysis, we identified a widely disrupted subnetwork with dominant connections involving the frontal lobe in patients with all-cause incident parkinsonism compared with those without at baseline. In addition, whole and regional brain network analysis indicated that decreased structural connectivity was closely associated with worse parkinsonian motor performance. Given SVD-related lesions are anatomically distributed throughout the whole brain, they are likely to predispose the brain to the disruption of white matter network (1). Besides MRI-visible lesions, MRI-invisible pathologies, for example, loss of microstructural integrity in normal-appearing white matter, probably further contribute to a more disconnected brain network (5,6). Therefore, global efficiency has been proposed as a sensitive proxy to capture brain pathological changes in SVD (38).

Motor performance is highly dependent on widespread interconnected brain networks (39), for example, interhemispheric connections of the corpus callosum, which are indispensable for coordinating and integrating complex motor programs, for example, gait, balance (40). de Laat et al. previously found that WMH and lacunes in the parietal and

frontal lobe were associated with an increased risk of mild parkinsonian signs (2). We extend this knowledge by showing that disrupted inter-hemispheric network architecture throughout the brain, mainly involving frontal and parietal lobes, contributes to parkinsonian signs. One might speculate that the basal ganglia-thalamo-frontal cortical circuits, which are crucial for neural control of movement, might be interrupted, leading to a reduction in the thalamocortical drive and subsequently parkinsonian signs, a preclinical level of parkinsonism (18). Besides, the parietal lobe, including supramarginal gyrus, superior parietal lobule, and inferior parietal lobule, is involved in parkinsonian signs. One may speculate these structural disconnections are interconnected with other cortical and subcortical regions through extensive neural networks to exert the effect on parkinsonian performance, for example, by integrating and synthesizing information from multi-modal inputs (41).

Another intriguing finding was that disrupted structural connectivity was associated with an increase of parkinsonian signs over time and future incident parkinsonism. Given brain topological changes might only become visible throughout long-term disease progression (38), this has important clinical relevance because network disruption, after taking into account the SVD burden, including PSMD as a sensitive DTI marker for SVD, may have the added value to serve as a useful marker to identify individuals at a higher risk of progressive parkinsonism in the long-term and predict the risk of conversion to incident parkinsonism. Also, the current finding might be generalized to the clinical care of older adults with late-life motor impairment. It is important to consider vascular risk factors in order to reduce the occurrence of future incident parkinsonism, as higher SVD burden is related to disrupted network connection and parkinsonism (42).

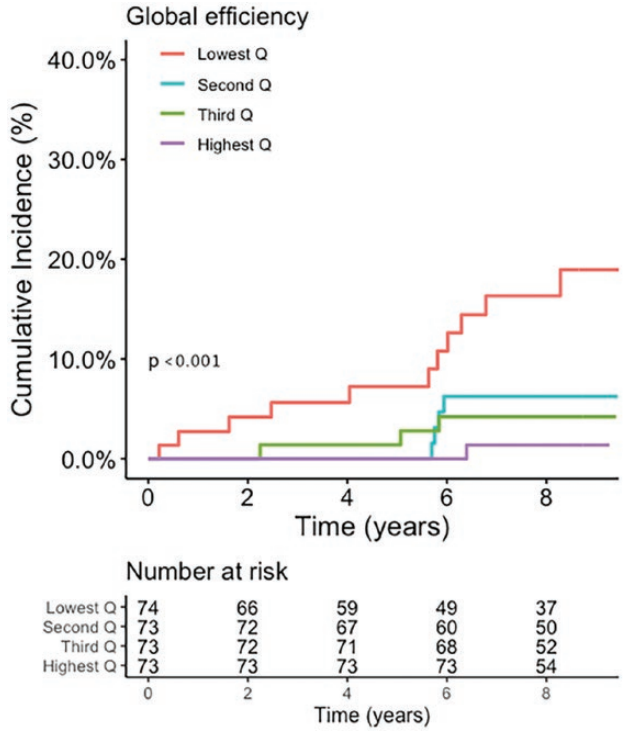

Figure 2. The cumulative risk for all-cause parkinsonism with respect to baseline global efficiency. The cumulative risk for all-cause parkinsonism is stratified by baseline global efficiency. Q = quartile.

Major strengths of the present study include the large cohort of participants covering a wide range of SVD spectrum. Furthermore, our longitudinal neuroimaging data in 2011 and 2015 were consistent, because they were acquired from the same scanner and protocol without upgrade or change. Of note, we intentionally did not adjust for vascular risk factors, because we considered them as a part of the causal chain between SVD and parkinsonism.

Several methodological limitations should be acknowledged. First, we have acquired relatively low-resolution images and the tractography algorithm might have a limited capacity to identify longer fibers and the inability to resolve crossing/kissing fibers. However, the streamlining algorithm is very reliable in terms of test–retest repeatability and computationally inexpensive to detect major white matter tracts (43). Second, this study is an observational study without intervention, future trials using brain network efficiency to detect treatment effects of motor disturbance are warranted. Third, we had a relatively small number of cases with incident parkinsonism, which may lead to lower statistical power, especially when including a certain number of predictors in the model. Studies with larger sample sizes to obtain a desirable number of incident events in the future are warranted to corroborate our main findings. Finally, although the PATCH algorithm is accurate and robust to correct motion artifacts, the DTI results may still be driven by residual motion artifacts. It should be noted that careful evaluation of motion artifacts in future research is warranted before drawing robust conclusions.

In conclusion, by utilizing network analysis based on diffusion tensor MRI, we found that global network efficiency is associated with a gradual decline in motor performance, ultimately leading to incident parkinsonism in the elderly with SVD. Our study supports the hypothesis that structural network disconnection attributable to SVD-related burden and MRI-invisible lesions are closely involved in the

Table 3. Baseline Global Efficiency, Its Changes Over Time and Risk of All-Cause Parkinsonism, Vascular Parkinsonism, and Parkinson's Disease on Top of Conventional SVD Markers

	All-Cause Parkinsonism			VaP			iPD		
Variables	HR	95% CI	*p* Value	HR	95% CI	*p* Value	HR	95% CI	*p* Value
Baseline GE	0.73	0.56 to 0.96	**.029**	0.58	0.40 to 0.84	**<.001**	1.09	0.66 to 1.79	.775
Delta GE	1.27	0.75 to 2.14	.381	1.33	0.68 to 2.59	.415	0.57	0.17 to 1.88	.233

Notes: All Fine-Gray sub-distribution hazard models were adjusted for age, sex, number of lacunes and microbleeds, white matter hyperintensity volume and total brain volume, UPDRS motor score in 2011. Death was treated as a competing risk. Bold values means significant statistically. CI = confidence interval; GE = global efficiency; HR = hazard ratio; SVD = small vessel disease; UPDRS = Unified Parkinson's Disease Rating scale.

pathophysiology of parkinsonism. Global network efficiency may have the potential to serve as a useful marker to capture changes in motor signs.

Supplementary Material

Supplementary data are available at *The Journals of Gerontology, Series A: Biological Sciences and Medical Sciences* online.

Funding

This work was supported by the Dutch Heart Foundation (grant 2016 T044 to A.M.T, grant 2014 T060 to FE.d.L) and the Netherlands CardioVascular Research Initiative: the Dutch Heart Foundation (CVON 2018-28 & 2012-06 Heart Brain Connection to A.M.T), VIDI innovational grant from The Netherlands Organization for Health Research and Development (ZonMw grant 016.126.351 to FE.d.L).

Conflict of Interest

None.

References

1. Ter Telgte A, van Leijsen EMC, Wiegertjes K, Klijn CJM, Tuladhar AM, de Leeuw F-E. Cerebral small vessel disease: from a focal to a global perspective. *Nat Rev Neurol*. 2018;14(7):387–398. doi:10.1038/s41582-018-0014-y
2. de Laat KF, van Norden AGW, Gons RAR, et al. Cerebral white matter lesions and lacunar infarcts contribute to the presence of mild Parkinsonian signs. *Stroke*. 2012;43(10):2574–2579. doi:10.1161/STROKEAHA.112.657130
3. van der Holst HM, van Uden IWM, Tuladhar AM, et al. Cerebral small vessel disease and incident parkinsonism: the RUN DMC study. *Neurology*. 2015;85(18):1569–1577. doi:10.1212/WNL.0000000000002082
4. van der Holst HM, Tuladhar AM, Zerbi V, et al. White matter changes and gait decline in cerebral small vessel disease. *Neuroimage Clin*. 2018;17:731–738. doi:10.1016/j.nicl.2017.12.007
5. Cai M, Jacob MA, Norris DG, Duering M, de Leeuw F-E, Tuladhar AM. Cognition mediates the relation between structural network efficiency and gait in small vessel disease. *NeuroImage: Clin*. 2021;30:102667. doi:10.1016/j.nicl.2021.102667
6. Cai M, Jacob MA, Norris DG, de Leeuw F-E, Tuladhar AM. Longitudinal relation between structural network efficiency, cognition, and gait in cerebral small vessel disease. *J Gerontol A Biol Sci Med Sci*. 2022;77(3):554–560. doi:10.1093/gerona/glab247
7. Boot EM, Leijsen E MC van, Bergkamp MI, et al. Structural network efficiency predicts cognitive decline in cerebral small vessel disease. *NeuroImage: Clin*. 2020;27:102325. doi:10.1016/j.nicl.2020.102325
8. Huo Y, Hong W, Huang J, et al. White matter hyperintensities and the progression from mild parkinsonian signs to parkinsonism and Parkinson's disease. *Neurobiol Aging*. 2020;96:267–276. doi:10.1016/j.neurobiolaging.2020.08.005
9. Zhang Y, Burock MA. Diffusion tensor imaging in Parkinson's disease and parkinsonian syndrome: a systematic review. *Front Neurol*. 2020;11:531993. doi:10.3389/fneur.2020.531993
10. Kok JG, Leemans A, Teune LK, et al. Structural network analysis using diffusion MRI tractography in Parkinson's disease and correlations with motor impairment. *Front Neurol*. 2020;11:841. doi:10.3389/fneur.2020.00841
11. Galantucci S, Agosta F, Stefanova E, et al. Structural brain connectome and cognitive impairment in Parkinson disease. *Radiology*. 2017;283(2):515–525. doi:10.1148/radiol.2016160274
12. Jacob MA, Cai M, Bergkamp M, et al. Cerebral small vessel disease progression increases risk of incident parkinsonism. *Ann Neurol*. 2023;93(6):1130–1141. doi:10.1002/ana.26615
13. van Norden AG, de Laat KF, Gons RA, et al. Causes and consequences of cerebral small vessel disease. The RUN DMC study: a prospective cohort study. Study rationale and protocol. *BMC Neurol*. 2011;11(1):29. doi:10.1186/1471-2377-11-29
14. Goetz CG, Stebbins GT, Chmura TA, Fahn S, Klawans HL, Marsden CD. Teaching tape for the motor section of the unified Parkinson's disease rating scale. *Mov Disord*. 1995;10(3):263–266. doi:10.1002/mds.870100305
15. Litvan I, Bhatia KP, Burn DJ, et al. SIC Task Force appraisal of clinical diagnostic criteria for parkinsonian disorders. *Mov Disord*. 2003;18(5):467–486. doi:10.1002/mds.10459
16. Louis ED, Luchsinger JA. History of vascular disease and mild parkinsonian signs in community-dwelling elderly individuals. *Arch Neurol*. 2006;63(5):717–722. doi:10.1001/archneur.63.5.717
17. Hughes AJ, Daniel SE, Kilford L, Lees AJ. Accuracy of clinical diagnosis of idiopathic Parkinson's disease: a clinico-pathological study of 100 cases. *J Neurol Neurosurg Psychiatry*. 1992;55(3):181–184. doi:10.1136/jnnp.55.3.181
18. Zijlmans JCM, Daniel SE, Hughes AJ, Révész T, Lees AJ. Clinicopathological investigation of vascular parkinsonism, including clinical criteria for diagnosis. *Mov Disord*. 2004;19(6):630–640. doi:10.1002/mds.20083
19. Fazekas F, Chawluk J, Alavi A, Hurtig H, Zimmerman R. MR signal abnormalities at 1.5 T in Alzheimer's dementia and normal aging. *Am J Roentgenol*. 1987;149(2):351–356. doi:10.2214/ajr.149.2.351
20. Cai M, Jacob MA, van Loenen MR, et al. Determinants and temporal dynamics of cerebral small vessel disease: 14-year follow-up. *Stroke*. 2022;53(9):2789–2798. doi:10.1161/STROKEAHA.121.038099
21. Wardlaw JM, Smith EE, Biessels GJ, et al. Neuroimaging standards for research into small vessel disease and its contribution to ageing and neurodegeneration. *Lancet Neurol*. 2013;12(8):822–838. doi:10.1016/S1474-4422(13)70124-8
22. Ghafoorian M, Karssemeijer N, van Uden IWM, et al. Automated detection of white matter hyperintensities of all sizes in cerebral small vessel disease: automated detection of white matter hyperintensities of all sizes. *Med Phys*. 2016;43(12):6246–6258. doi:10.1118/1.4966029
23. van Leijsen EMC, van Uden IWM, Ghafoorian M, et al. Nonlinear temporal dynamics of cerebral small vessel disease: the RUN DMC study. *Neurology*. 2017;89(15):1569–1577. doi:10.1212/WNL.0000000000004490
24. Manjón JV, Coupé P, Concha L, Buades A, Collins DL, Robles M. Diffusion weighted image denoising using overcomplete local PCA. *PLoS One*. 2013;8(9):e73021. doi:10.1371/journal.pone.0073021
25. Zwiers MP. Patching cardiac and head motion artefacts in diffusion-weighted images. *Neuroimage*. 2010;53(2):565–575. doi:10.1016/j.neuroimage.2010.06.014
26. Smith SM, Jenkinson M, Woolrich MW, et al. Advances in functional and structural MR image analysis and implementation as FSL. *Neuroimage*. 2004;23:S208–S219. doi:10.1016/j.neuroimage.2004.07.051
27. Lawrence AJ, Chung AW, Morris RG, Markus HS, Barrick TR. Structural network efficiency is associated with cognitive impairment in small-vessel disease. *Neurology*. 2014;83(4):304–311. doi:10.1212/WNL.0000000000000612
28. Tzourio-Mazoyer N, Landeau B, Papathanassiou D, et al. Automated anatomical labeling of activations in SPM using a macroscopic anatomical parcellation of the MNI MRI single-subject brain. *Neuroimage*. 2002;15(1):273–289. doi:10.1006/nimg.2001.0978
29. Jenkinson M, Bannister P, Brady M, Smith S. Improved optimization for the robust and accurate linear registration and motion correction of brain images. *Neuroimage*. 2002;17(2):825–841. doi:10.1016/s1053-8119(02)91132-8
30. Avants BB, Tustison NJ, Song G, Cook PA, Klein A, Gee JC. A reproducible evaluation of ANTs similarity metric performance

in brain image registration. *Neuroimage*. 2011;54(3):2033–2044. doi:10.1016/j.neuroimage.2010.09.025
31. Hagmann P, Kurant M, Gigandet X, et al. Mapping human whole-brain structural networks with diffusion MRI. *PLoS One*. 2007;2(7):e597. doi:10.1371/journal.pone.0000597
32. Lawrence AJ, Zeestraten EA, Benjamin P, et al. Longitudinal decline in structural networks predicts dementia in cerebral small vessel disease. *Neurology*. 2018;90(21):e1898–e1910. doi:10.1212/WNL.0000000000005551
33. de Brito Robalo BM, Vlegels N, Meier J, Leemans A, Biessels GJ, Reijmer YD. Effect of fixed-density thresholding on structural brain networks: a demonstration in cerebral small vessel disease. *Brain Connect*. 2020;10(3):121–133. doi:10.1089/brain.2019.0686
34. Achard S, Bullmore E. Efficiency and cost of economical brain functional networks. *PLoS Comput Biol*. 2007;3(2):e17. doi:10.1371/journal.pcbi.0030017
35. Tuladhar AM, Reid AT, Shumskaya E, et al. Relationship between white matter hyperintensities, cortical thickness, and cognition. *Stroke*. 2015;46(2):425–432. doi:10.1161/STROKEAHA.114.007146
36. Baykara E, Gesierich B, Adam R, et al. A novel imaging marker for small vessel disease based on skeletonization of white matter tracts and diffusion histograms: novel SVD imaging marker. *Ann Neurol*. 2016;80(4):581–592. doi:10.1002/ana.24758
37. Austin PC, Fine JP. Practical recommendations for reporting Fine-Gray model analyses for competing risk data. *Stat Med*. 2017;36(27):4391–4400. doi:10.1002/sim.7501
38. Dewenter A, Gesierich B, ter Telgte A, et al. Systematic validation of structural brain networks in cerebral small vessel disease. *J Cereb Blood Flow Metab*. 2021;42:1020–1032. doi:10.1177/0271678x211069228
39. de Laat KF, van Norden AGW, Gons RAR, et al. Gait in elderly with cerebral small vessel disease. *Stroke*. 2010;41(8):1652–1658. doi:10.1161/STROKEAHA.110.583229
40. Bohnen NI, Albin RL. White matter lesions in Parkinson disease. *Nat Rev Neurol*. 2011;7(4):229–236. doi:10.1038/nrneurol.2011.21
41. Garey LJ. Cortex cerebri. performance, structural and functional organization of the cortex. *Trends Neurosci*. 1996;19(7):300–301. doi:10.1016/s0166-2236(96)60018-6
42. Oveisgharan S, Yu L, Poole VN, et al. Association of white matter hyperintensities with pathology and progression of parkinsonism in aging. *JAMA Neurol*. 2021;78(12):1494–1502. doi:10.1001/jamaneurol.2021.3996
43. Mori S, van Zijl PCM. Fiber tracking: principles and strategies—a technical review. *NMR Biomed*. 2002;15(7–8):468–480. doi:10.1002/nbm.781